Differences in the Evolution of Ouabain-Induced Stroke Between Immunocompetent and Immunodeficient Mice as Detected by T2-weighted MRI

Agatha Lyczek[1,2], Miroslaw Janowski[1,2], Jinyuan Zhou[1,3], Jiadi Xu[1,3], Peter PC van Zijl[1,3], Jeff WM Bulte[1,2], and Piotr Walczak[1,2]

[1]Radiology and Radiological Science, Johns Hopkins University, Baltimore, MD, United States, [2]Institute for Cell Engineering, Johns Hopkins University, Baltimore, MD, United States, [3]F. M. Kirby Research Center for Functional Brain Imaging, Kennedy Krieger Research Institute, Baltimore, MD, United States

Introduction: Ischemic stroke is the leading cause of long-term, severe disability in the United States and Europe, and a major cause of death worldwide. It was recently shown that immunological and inflammatory processes, manifested by leukocyte trafficking into the central nervous system, contribute substantially to secondary brain damage, exacerbating the follow-up effects of ischemia. Consequently, there is increasing interest in characterizing the inflammatory response to ischemia, and identifying new therapeutic approaches. Recently, it was shown that immunomodulatory therapy preventing lymphocytes from invading into the brain reduces post-ischemic brain injury (1). This suggests that immunotherapy may be a promising neuroprotective approach for stroke. To date, little is known about the dynamics of ischemia evolution in immunodeficient animals. A detailed, longitudinal analysis and comparison of ischemic lesion evolution in immunocompetent vs. immunodeficient mice would provide important insight into the role of the immune response in stroke pathogenesis. Here, we used serial MRI to characterize the evolution of ouabain-induced stroke (2) in immunocompetent (*balb/c*) vs. immunodeficient (*rag2-/-)* mice.

Materials and Methods: *Ouabain model of stroke*: The experiments were performed on adult *rag2-/-* and *balb/c* mice (n=3 each). Mice were immobilized in a stereotactic apparatus. A small hole was drilled in the cranium over the right hemisphere. A needle was lowered into the striatum (coordinates A 0.5, L 2.2, D 2.4 mm) and 0.5 µl of 5 mMol ouabain solution (Sigma) was injected into the brain at a rate of 0.5 µl/min.
MRI: The mice were placed in a custom-built probe equipped with an isoflurane anesthesia delivery system, with temperature and respiratory control, and imaged using an horizontal 11.7T Biospec system (Bruker BioSpin) with a 16 cm diameter bore magnet. Transmission was achieved using a quadrature volume resonator and a 2x2 mouse surface coil array was used for signal detection. T2-w images were acquired using an MSME sequence with the following parameters: TE=10,20,30,40,50,60,70,80,90, and 100 ms; TR=6000 ms; NAV=1, matrix=128x96 pixels; FOV=13x11 mm^2; scan time=10 min. T2 values were calculated for regions of interest within the cortex (CTX), corpus callosum (CC), and striatum (STR) for the lesion and contralateral hemisphere using Paravision 5.1.
Statistical Analysis: The lowest means square (LMS) test was incorporated into PROC MIXED software (SAS). The level of statistical significance was set at p=0.05.

Results: One day after lesion induction, T2-w MRI showed distinct hyperintensity in both immunocompetent (*balb/c,* **Fig. A**) and immunodeficient (*rag2-/-,* **Fig. C**) mice in all animals. Hyperintensities were observed throughout the cortex, corpus callosum, and striatum (**Fig. A, white, black, and gray arrowheads, respectively)**. The lesion sizes and T2 values in both *balb/c* and *rag2-/-* mice were similar at Day 1 (acute lesion) (**Figs. C and F, respectively, P=0.4**), but significantly different at Day 5. In *balb/c* mice, five days after stroke induction, the lesion consolidated and its volume increased (**Fig. B**). At both time points, T2 values within the lesion were significantly longer than those on the contralateral side **(Fig. C, *P <0.0001 for both day one, and day five**). The change in T2 of the lesioned area within the *balb/c* brains was not significant between these time points (**P=0.9**). In contrast, intriguingly, MRI of the *rag2-/-* mice at the five-day time-point revealed much smaller hyperintense regions (**Fig. E, *P<0.0001 white arrow**). T2 measurements in *rag2-/-* animals showed significantly increased values within the lesion for day one, compared to values in the contralateral hemisphere (**Fig. F, *P <0.0001**). On day five, however, T2 values for the lesion were only slightly elevated, when compared to the contralateral hemisphere, although the difference was significant (***P=0.02**). Further analysis of individual brain structures revealed that the T2 of both gray matter structures (cortex and striatum) returned to the level of the contralateral hemisphere, indicating recovery (**P=0.56** and **P=0.43**, respectively, but T2 for white matter (corpus callosum) was still substantially longer (**P=0.006**).

Conclusion: MRI is well suited to monitor differences in the evolution of stroke between immunocompetent and immunodeficient animals. Our results indicate that an inflammatory response contributes very rapidly (as early as 5 days) to the deleterious effects of stroke. Imaging of *rag2-/-* mice showed substantial recovery at 5 days, suggesting that the neurons may be capable of surviving the acute phase of stroke, provided that no inflammatory insult follows. In *rag2-/-* mice, T2 abnormalities persisted within the corpus callosum, the largest white matter structure in the brain, suggesting that perhaps oligodendrocytes are more sensitive to the primary hypoxic insult. Thus, perhaps the recommended therapy for ischemic stroke should be a combination of immunomodulation and strategies aimed at restoration of myelinating glia. Further histological studies are in progress to correlate MR imaging observations with cellular and molecular events.

Funding Support: MSCRFII-0193; MSCRFII0052, NIH/NCRR1S10RR028955-01

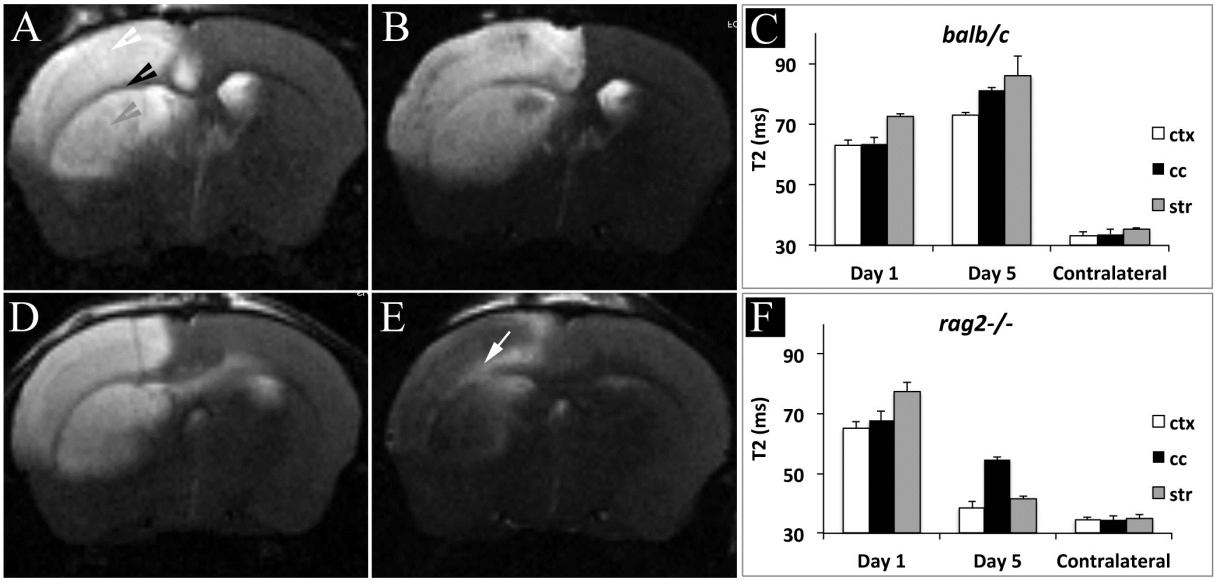

References:

1 Arthur Liesz, Roland Veltkamp, et al. Inhibition of lymphocyte trafficking shields the brain against deleterious neuroinflammation after stroke, Brain (2011) 134 (3): 704-720.doi: 10.1093/brain/awr008

2 Janowski M, Gornicka-Pawlak E, Kozlowska H, Domanska-Janik K, Gielecki J, Lukomska B. Structural and functional characteristic of a model for deep-seated lacunar infarct in rats, J Neurol Sci (2008), doi: 10.1016/j.jns.2008.06.019